ACS Catalysis

Research Article

pubs.acs.org/acscatalysis

Iodine Catalyzed Propane Oxidative Dehydrogenation Using Dibromomethane as an Oxidant

Kunlun Ding,[†] Aihua Zhang,[‡] and Galen D. Stucky*,[†]

[†]Department of Chemistry and Biochemistry, University of California, Santa Barbara, California 93106-9510, United States

[‡]Gas Reaction Technologies, Inc., 861 Ward Drive, Santa Barbara, California 93111, United States

Supporting Information

ABSTRACT: Propane oxidative dehydrogenation is a promising candidate for on-purpose propylene production. However, in oxidative dehydrogenation the propylene yield is limited by the simultaneous oxidization of propane to multiple oxygenated byproducts. We show that a small amount of I_2 is highly effective in catalyzing the dehydrogenation of propane into propylene, using dibromomethane (DBM), a byproduct of the activation of methane by bromine, as the oxidant. Single-pass "C_3H_6+C_3H_7X" (X = Br, I; C_3H_7X can be easily converted to C_3H_6 and HX) yields of up to 80% can be easily achieved, with the highly selective conversion of DBM to methyl bromide, which is readily converted into either high-market-value petrochemicals or liquid fuels. Bearing in mind that the formation of DBM is one of the major undesirable byproducts in the bromine-mediated gas-to-liquid technology, our findings create a win-win situation. On the one hand, this approach is promising for developing a low-cost, on-purpose propylene technology using natural gas as a feedstock. On the other hand, DBM is shown to be a useful reactant for the industrial application of the bromine-mediated gas-to-liquid technology.

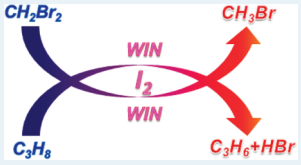

KEYWORDS: *on-purpose propylene, oxidative dehydrogenation, gas-to-liquid, iodine, dibromomethane*

INTRODUCTION

Driven by the commercial demand for polypropylene, the propylene market is increasing rapidly. Approximately two-thirds of current propylene production is supplied from steam cracking of liquid feedstocks (primarily naphtha), and the balance is supplied mostly from fluidic catalytic cracking. However, in both steam cracking and fluidic catalytic cracking, propylene is produced as a byproduct, and the selectivity for its synthesis is always low. As a result of the build-up of ethane-based crackers, the ratio of propylene/ethylene produced from steam crackers is anticipated to fall. Meanwhile, the demand ratio of propylene/ethylene is increasing. As a result there is a growing gap between propylene demand and propylene supplied from steam crackers. For this reason, it becomes increasingly important to develop on-purpose propylene production technologies that offer higher propylene/ethylene production ratios.[1]

Among different on-purpose propylene technologies, propane dehydrogenation is promising because of the theoretical high propylene selectivity and low capital investment, and does not depend on the cost of naphtha. Propane is commercially available from two major sources, petroleum refining and natural gas processing (natural gas usually contains 1−4% of propane by volume[2,3]). However, limited by thermodynamics, the single-pass conversion of propane to propylene by dehydrogenation is low unless a very high reaction temperature (~1000 K) is applied. Introducing an oxidant can drive the reaction to be more thermodynamically favorable. Unfortunately, the highest propylene yield reported for propane oxidative dehydrogenation (ODH) is only about 30%.[4−6] The most important reason for this low yield is that the allyl C−H bond is much weaker than the C−H bonds in propane, which leads ultimately to consecutive oxidation to CO_x.[5] Milder oxidants such as CO_2 and NO_x have been studied.[7−9] While propylene selectivity is increased, catalyst activity and durability are largely compromised. Small amounts of halogens or halo-compounds have been shown to promote propane conversion and propylene selectivity in oxygen mediated propane ODH.[10−12] However, propylene yield is still very low.

Using halogens alone as oxidants, propylene can be produced either directly by halo-dehydrogenation or from a subsequent hydrogen halide elimination step from propyl halides. However, analogous to the successive oxidation of propane with oxygen, the halogen (F_2, Cl_2, and Br_2) reactions with alkanes are fast and nonselective, so that single-pass yields are limited in the conversion of propane to propyl halides and subsequently to propylene. I_2 reacts selectively, but relatively slowly, with propane at low temperatures to produce propyl iodides and propylene.[13,14] High propylene yields can be achieved with stoichiometric I_2 and propane feeding. However, this reaction is only thermodynamically favorable at high temperatures (above 750 K). Furthermore, the stoichiometric reaction of I_2 with propane is needed. The recycling efficiency of the relatively expensive I_2 greatly hinders the industrial application of this process.[11,15]

It is important to note that for methane, the halogen conversion of methane to higher hydrocarbons can be used instead of the highly energy-consuming synthesis gas process.[16,17] Methyl halides have been shown to be directly transformed into olefins or higher hydrocarbons by coupling processes analogous

Received: February 27, 2012
Revised: April 12, 2012
Published: May 2, 2012

   dx.doi.org/10.1021/cs3001418 | ACS Catal. 2012, 2, 1049−1056

to the methanol-to-olefins and methanol-to-gasoline processes over either zeolites or bifunctional acid-base metal oxides.[18−20] Of the halogens, bromine has the advantages that the selectivity for methyl bromide is relatively high; and, the C−Br bond is weak enough to allow for facile bromine removal and recovery for reuse in a closed reaction cycle for the conversion of methane to liquid fuels or olefins.[16,17] However, since dibromomethane (DBM) is the main byproduct in the methane bromination process and cokes heavily over zeolite catalysts, a significant chemical challenge is to improve the selectivity for methyl bromide versus that for DBM at high conversion.[21] Putting together the increasing propylene demands and the DBM issue of bromine mediated stranded natural gas conversion to liquid fuels, reacting propane and DBM to produce propylene and methyl bromide will create a win-win situation. However, although this reaction is thermodynamically favorable (Supporting Information, Figure S1), it is difficult to find an efficient heterogeneous catalyst (Supporting Information, Figure S2). One main reason for this is that DBM tends to decompose into coke and HBr on solid catalysts, leaving unreacted propane.

In this Article we show that a small amount of I_2 is highly effective in catalyzing the gas phase reaction between propane and DBM:

$$C_3H_8 + CH_2Br_2 \rightarrow C_3H_6 + HBr + CH_3Br \qquad \text{(rxn. 1)}$$

Single-pass "C_3H_6+C_3H_7X" yields up to 80% can be easily achieved, and DBM selectively converts (>90%) to methyl bromide. Our findings are promising for developing a low-cost on-purpose propylene technology using natural gas as feedstock. In addition, by means of this reaction we are able to effectively utilize DBM that is generated as part of bromine-mediated Gas-To-Liquid (GTL) technology.

EXPERIMENTAL SECTION

The reactions were conducted in an atmospheric pressure glass tube reactor system. The configuration of the reaction system is shown in Figure 1. C_3H_8, HBr, and Ar flow rate was controlled

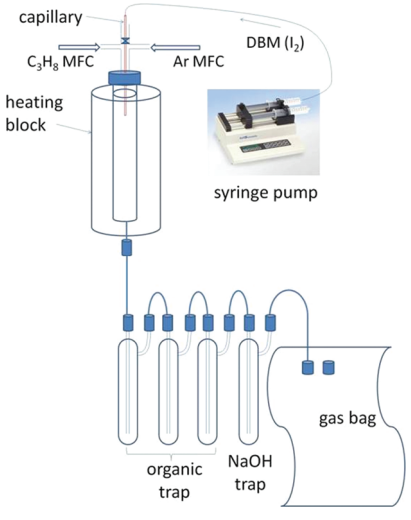

Figure 1. Configuration of the reaction system (CH_2Br_2 + C_3H_8 → products).

by mass flow controller (MFC). I_2 was dissolved in DBM and delivered by syringe pump. DBM(I_2) was vaporized in the head space of the reactor. The effluent stream from the reactor was passed through a series of glass bubbler traps containing organic solution (10 wt % octadecane in hexadecane); all remaining gaseous product were collected in a gas bag after passing through a final base trap (4 M NaOH solution) to prevent any residual HBr from entering the bag. For most of the experiments, reactions were run for half an hour with all the products collected and analyzed. The products were analyzed with three GCs, which measured: (1) CH_3Br; (2) gaseous hydrocarbon products C_1−C_6; and (3) unconverted DBM and liquid halocarbon products. All the experiments reported here had carbon balances of 95−105%. Isotope tracing experiments were characterized by GC-MS, and the H/D distribution patterns were deconvoluted based on standard MS spectra from NIST database (http://webbook.nist.gov/chemistry).

RESULTS AND DISCUSSION

Figure 2 shows the reaction temperature profiles of propane and DBM conversion in the presence of different amounts of I_2. All the conversions increase exponentially with reaction temperature. The bottom curve belongs to that without I_2, and shows that propane and DBM conversion are only 11.6% and 12.1% at 798 K. Introducing 1% of $I_2/(CH_2Br_2 + I_2)$ leads to approximately a 200% increase in both propane and DBM conversion. These conversions increase with the mole ratio of $I_2/(CH_2Br_2 + I_2)$, to 74.4% and 74.8% at 798 K using 5% of $I_2/(CH_2Br_2 + I_2)$, for propane and DBM. Different residence times were also studied, and the conversions are given in Figure 2. Longer residence time leads to higher conversion. The highest conversions for propane and DBM (87.4% and 91.1%) were obtained at 798 K with a 16 s residence time.

Typical product distributions are given in Figure 2 and Supporting Information, Figures S3 to S5. In the presence of I_2, C_3H_6 is the main product from C_3H_8, together with small amounts of C_3H_7Br and C_3H_7I. The formation of C_3H_7X can be partially attributed to the addition reactions of C_3H_6 + HX, which might occur either in the gas phase or in the organic trap. Using NaOH aqueous solution/organic biphase trap significantly suppresses the formation of C_3H_7Br, suggesting that C_3H_7Br formation mostly took place in the trap. C_3H_7I can be generated by the C_3H_6 + HI addition reaction in the cooled outlet stream or might originate from the nondecomposed intermediate. CH_3Br is the most abundant product obtained from DBM reactant. The selectivities toward C_3H_5Br (BrCH═$CHCH_3$ and CH_2═$CBrCH_3$) and CH_4 increase with reaction temperature and residence time (Supporting Information, Figures S4 and S5). However, these selectivities are still far less than those of the main products even when as high as 90% propane and DBM conversions are achieved. Since C_3H_7Br and C_3H_7I can eliminate HBr and HI and produce propylene easily over certain heterogeneous surfaces,[22,23] it is reasonable to include C_3H_7X as part of the propylene production. The highest "C_3H_6+C_3H_7X" yield is approximately 80% (798 K, 16 s). As the propane and DBM conversions are almost equal, we can conclude that propane and DBM reacts stoichiometrically via rxn. 1 in the presence of I_2.

To elucidate the reaction mechanism between propane and DBM in the presence of I_2, the following control experiments were carried out. All of these experiments were run at 773 K using identical DBM partial pressures (7/61) and residence times (8 s). In "DBM + Ar" experiment, 8.9% of the DBM was converted to CH_3Br and $CHBr_3$ with almost equal selectivities (Supporting Information, Figure S6A). HBr cofeeding greatly increased the DBM conversion to 32.2%. The CH_3Br selectivity was slightly higher than that of $CHBr_3$ in the presence of HBr (Supporting Information, Figure S6B), suggesting that small amounts of Br_2 should be formed. This was confirmed by the

dx.doi.org/10.1021/cs3001418 | ACS Catal. 2012, 2, 1049−1056

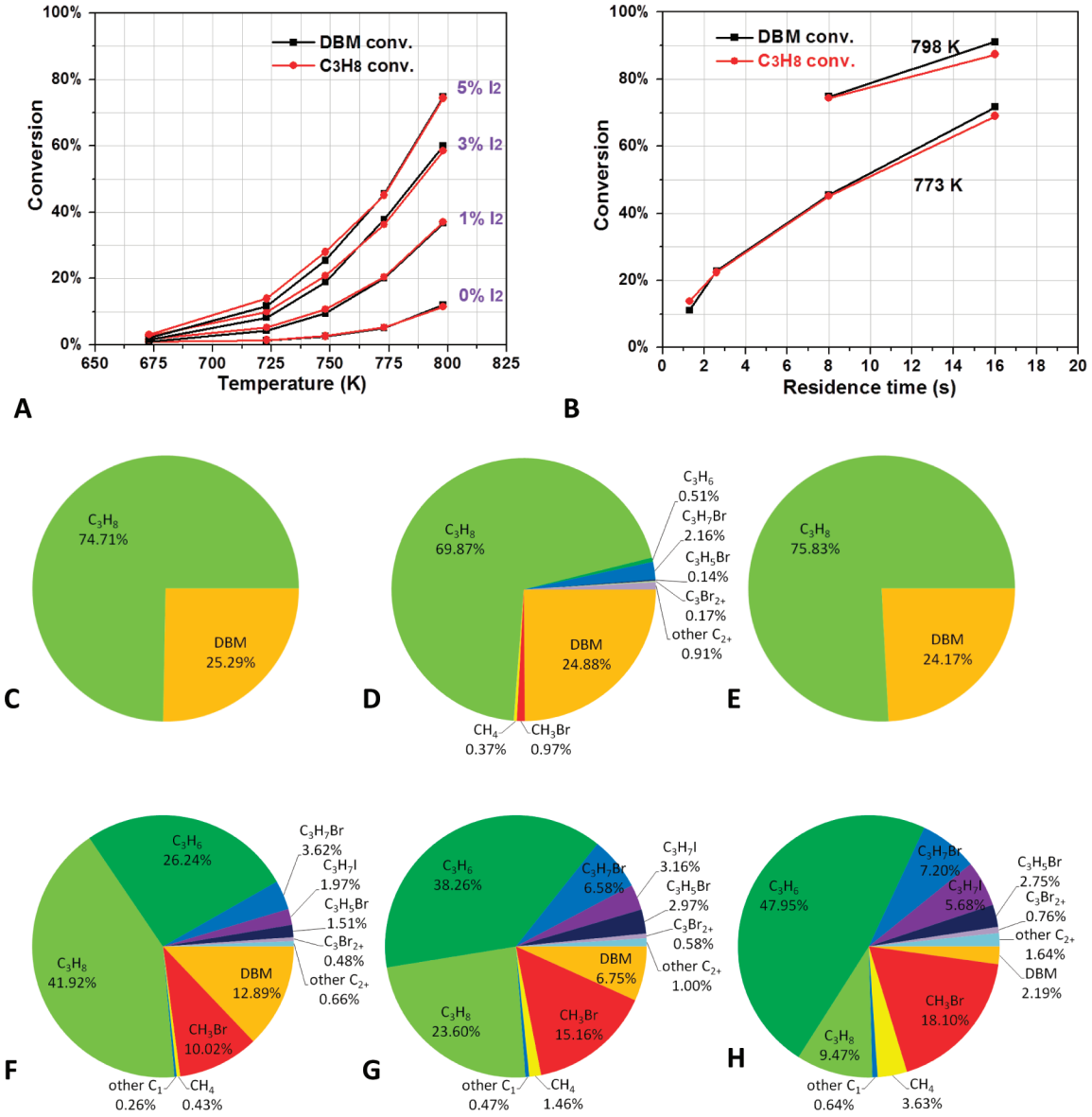

Figure 2. (A) Temperature-dependent conversions of the "C_3H_8 + CH_2Br_2" reaction with different mole ratios of $I_2/(CH_2Br_2 + I_2)$ (τ = 8 s, CH_2Br_2/C_3H_8/HBr/Ar mole ratio of 7:7:14:33, C_3H_8 input 8.2 mmol); (B) Residence-time-dependent conversions of the "C_3H_8 + CH_2Br_2" reaction at different reaction temperatures (5% of $I_2/(CH_2Br_2+I_2)$, CH_2Br_2/C_3H_8/HBr/Ar mole ratio of 7:7:14:33, C_3H_8 input 8.2 mmol); (C) Inlet gas composition and (D) product distribution of the "C_3H_8 + CH_2Br_2" reaction without I_2 (773 K, τ = 8 s, CH_2Br_2/C_3H_8/HBr/Ar mole ratio of 7:7:14:33, C_3H_8 input 8.2 mmol); (E) Inlet gas composition and (F–H) product distributions of the "C_3H_8 + CH_2Br_2" reaction with 5% of $I_2/(CH_2Br_2 + I_2)$ ((F) 773 K, τ = 8 s; (G) 773 K, τ = 16 s; (H) 798 K, τ = 16 s; CH_2Br_2/C_3H_8/HBr/Ar mole ratio of 7:7:14:33, C_3H_8 input 8.2 mmol). "τ" denotes residence time; all the pie charts are on a mole carbon basis.

trap color changing from colorless to brown-red. In the presence of HBr, once the $\bullet CH_2Br$ radical is generated (rxn. 2), it will react with HBr (rxn. 3) quickly. Thus the recombination of $\bullet CH_2Br$ radical and $\bullet Br$ radical is suppressed. The $\bullet Br$ radical can abstract either Br or H from DBM according to rxn. 4 and rxn. 5.

$$CH_2Br_2 \leftrightarrows \bullet CH_2Br + \bullet Br \quad \text{(rxn. 2)}$$

$$\bullet CH_2Br + HBr \leftrightarrows \bullet Br + CH_3Br \quad \text{(rxn. 3)}$$

$$\bullet Br + CH_2Br_2 \leftrightarrows \bullet CH_2Br + Br_2 \quad \text{(rxn. 4)}$$

$$\bullet Br + CH_2Br_2 \leftrightarrows \bullet CHBr_2 + HBr \quad \text{(rxn. 5)}$$

$$\bullet CHBr_2 + Br_2 \leftrightarrows \bullet Br + CHBr_3 \quad \text{(rxn. 6)}$$

$$\bullet Br + \bullet Br + M \leftrightarrows Br_2 + M \quad \text{(rxn. 7)}$$

Combination of rxn. 3 and rxn. 4 constructs an overall reaction of

$$CH_2Br_2 + HBr \leftrightarrows CH_3Br + Br_2 \quad \text{(rxn. 8)}$$

Combination of rxn. 3, rxn. 4, rxn. 5, and rxn. 6 constructs an overall reaction of

$$2CH_2Br_2 \leftrightarrows CH_3Br + CHBr_3 \quad \text{(rxn. 9)}$$

The $\bullet Br$ radical can promote both rxn. 8 and rxn. 9. The former generates Br_2, and then increases the $\bullet Br$ radical concentration via rxn. 7, thus further accelerating the DBM conversion via rxn. 8 and rxn. 9. Without the cofeeding of HBr, rxn. 9 instead of rxn. 8 makes a significant contribution to the DBM reactions

dx.doi.org/10.1021/cs3001418 | ACS Catal. 2012, 2, 1049–1056

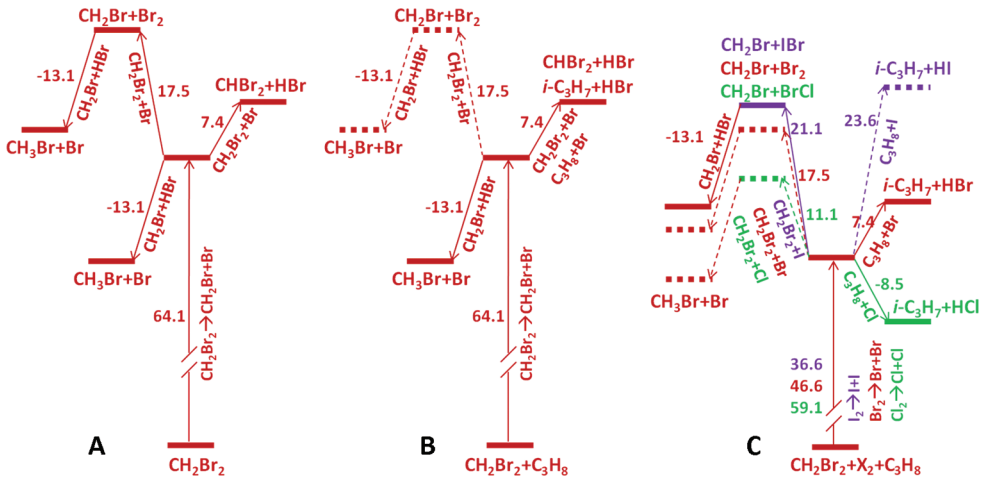

Figure 3. Energy profiles (at 800 K) of (A) "DBM + HBr + Ar" system, (B) "DBM + C_3H_8 + HBr + Ar" system and (C) "DBM + C_3H_8 + X_2 + HBr + Ar" (X = Cl, Br, and I) systems. (Energy barriers for all the H-abstraction from HBr and HI, and halogen-abstraction from Br_2, I_2, and IBr are close to zero, unless otherwise mentioned.).

("DBM + Ar" system). With the cofeeding of HBr, rxn. 8 and rxn. 9 both contribute to the DBM reactions ("DBM + HBr + Ar" system). Synergistically, HBr cofeeding leads to a higher ratio of $CH_3Br/CHBr_3$, as well as the formation of Br_2, and the formation of Br_2 further accelerates the DBM conversion. Figure 3A shows the energy profile of the "DBM + HBr + Ar" system.

Comparing the "DBM + HBr + Ar" system and the "DBM + C_3H_8 + HBr + Ar" system, the introduction of C_3H_8 in the latter system greatly suppresses the DBM conversion (Figures 2 and Supporting Information, Figure S6). The energy profile of the "DBM + C_3H_8 + HBr + Ar" system is given in Figure 3B. Most of the rate constants are listed in Supporting Information, Table S1. However, since most rate constants available in the literature were measured in the temperature region of 300−600 K, extending the Arrhenius equation to 800 K may cause certain deviations. Being aware of the possible deviations, here we only compare the rate constants that have great differences. Hereafter, k_n and k_{-n} denote the rate constant of forward and backward reaction of rxn. n, respectively. From Supporting Information, Table S1 we can know that the rate constant of $k_{10} \gg k_4 + k_5$, which means most of the •Br radicals are consumed by C_3H_8 via rxn. 10 and rxn. 11; thus, the •Br radical catalyzed DBM conversion is suppressed.

$$\bullet Br + C_3H_8 \leftrightarrows \bullet C_3H_7 + HBr \qquad \text{(rxn. 10)}$$

$$\bullet Br + \bullet C_3H_7 \leftrightarrows C_3H_7Br \qquad \text{(rxn. 11)}$$

For the same reason, the addition of Br_2 to the "DBM + C_3H_8 + HBr + Ar" system only increases the C_3H_8 conversion, but not the DBM conversion. The energy profiles of the "DBM + C_3H_8 + X_2 + HBr + Ar" (X = Cl, Br, and I) systems are given in Figure 3C. The energy profiles show that Cl_2 is not as favorable a reactant as Br_2, because the reaction between Cl_2 and C_3H_8 proceeds much more easily than that between Br_2 and C_3H_8. In addition, in the presence of I_2, Br-abstraction is comparatively easier than H-abstraction, so that I_2 will contribute more to Br-abstraction from DBM than H-abstraction from C_3H_8. Once •CH_2Br and •Br are formed, the former will evolve into CH_3Br quickly, while •Br will dehydrogenate C_3H_8.

Complete reaction pathways as well as the energy profile for the "C_3H_8 + DBM + I_2 + HBr + Ar" system are illustrated in Figure 4A. (1) The first step includes the fast equilibrium of I_2 dissociation and its recombination;[24,25]

$$I_2 + M \leftrightarrows \bullet I + \bullet I + M \qquad \text{(rxn. 12)}$$

(2) the dissociated •I radical abstracts Br from DBM, generating •CH_2Br and IBr;

$$\bullet I + CH_2Br_2 \leftrightarrows \bullet CH_2Br + IBr \qquad \text{(rxn. 13)}$$

(3) •CH_2Br abstracts H from HBr through rxn. 3, forming •Br and a final product CH_3Br; (4) •Br abstracts H from C_3H_8 through rxn. 10, forming HBr and •C_3H_7; (5) •C_3H_7 is trapped by I_2, generating C_3H_7I and •I;

$$\bullet C_3H_7 + I_2 \leftrightarrows \bullet I + C_3H_7I \qquad \text{(rxn. 14)}$$

(6) C_3H_7I is very unstable at high temperature and quickly decomposes into C_3H_6 and HI;[24]

$$C_3H_7I \leftrightarrows C_3H_6 + HI \qquad \text{(rxn. 15)}$$

Instead of step 5 and step 6, another way to generate C_3H_6 and HI is through rxn. 16.[14]

$$\bullet C_3H_7 + \bullet I \leftrightarrows C_3H_6 + HI \qquad \text{(rxn. 16)}$$

(7) HI reacts with •Br, regenerating •I.

$$\bullet I + IBr \leftrightarrows \bullet Br + I_2 \qquad \text{(rxn. 17)}$$

$$\bullet Br + HI \leftrightarrows \bullet I + HBr \qquad \text{(rxn. 18)}$$

Generally speaking, the entire process starts with a fast pre-equilibrium (rxn. 12), followed by a rate-determining step of Br abstraction from DBM by •I radical (rxn. 13), ending with several fast sequential reactions that generate the final products CH_3Br, C_3H_6, and HBr, and regenerating the •I radicals and I_2. The two most important roles of iodine in the entire process are abstracting bromine from DBM and serving as a radical trap for all the radicals. Bromine, instead of iodine, contributes the most to the actual propane dehydrogenation.

The reaction rate can be written as

$$r = k_{13}[\bullet I][CH_2Br_2] \qquad \text{(eq. 1)}$$

Since rxn. 12 is a fast equilibrium and the equilibrium constant $K_{12} \ll 1$, we know that

$$[\bullet I] \approx A_{12}\sqrt{K_{12}}\sqrt{[I_2]} = A'_{12}\exp[-\Delta H_{12}/2RT]\sqrt{[I_2]} \qquad \text{(eq. 2)}$$

dx.doi.org/10.1021/cs3001418 | ACS Catal. 2012, 2, 1049−1056

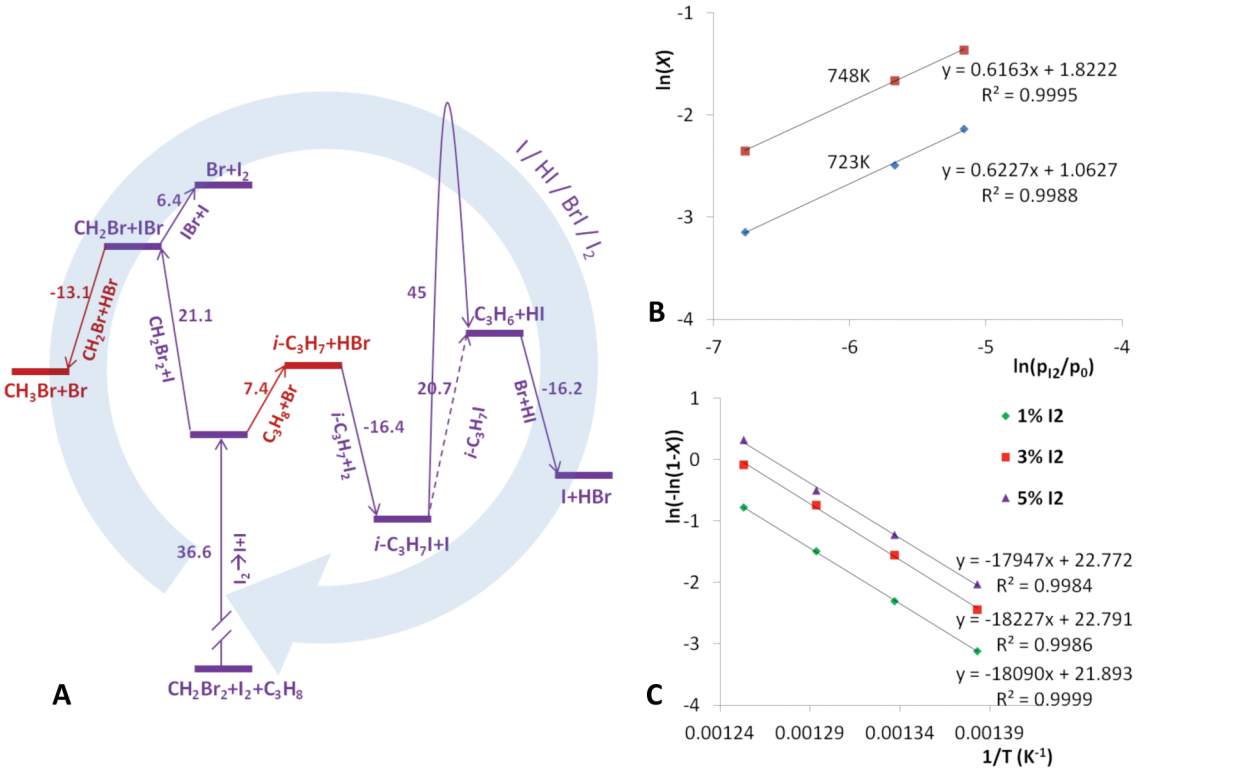

Figure 4. (A) Reaction pathways and also the energy profile (at 800 K) for "DBM + C_3H_8 + I_2 + HBr + Ar" system; (B) Plots of ln(X) against ln(p_{12}/p_0) at 723 K and 748 K; (C) Arrhenius plots based on the DBM conversions at different reaction temperatures with different mole ratios of $I_2/(CH_2Br_2 + I_2)$.

where A_{12} and A'_{12} are temperature-independent values and ΔH_{12} is the enthalpy change of rxn. 12. Combining eq. 1 and eq. 2, we know that at the same temperature, the initial DBM converting rate follows

$$\ln(r_0) = 0.5\ln([I_2]) + \text{constant} \qquad \text{(eq. 3)}$$

The initial DBM converting rate can be roughly calculated at low conversions. In Figure 4B, we plot ln(X) against ln(p_{12}/p_0) at the reaction temperatures of 723 K and 748 K (DBM conversions are lower than 25%); the slopes are both 0.6, which is close to the theoretical value of 0.5. The deviation might derive from the approximations. Mathematical analysis (Supporting Information, Figure S7) of the reaction kinetics suggests that the DBM converting rate is proportional to the first power of $[CH_2Br_2]$, which further supports our proposed rate law.

Assuming [•I] is in steady state and does not vary with the reaction, the following equation is produced by the integration of eq. 1,

$$-\ln(1 - X) = k_{13}[\bullet I]t = A_{13}\exp[-E_{a13}/RT][\bullet I]t \qquad \text{(eq. 4)}$$

where X is the DBM conversion, k_{13} is the rate constant of rxn. 13, t is the reaction time, and A_{13} and E_{a13} are the pre-exponential factor and the activation energy of rxn. 13. We substitute eq. 2 into eq. 4, giving

$$\ln(-\ln(1 - X)) = -\frac{E_{a13} + \Delta H_{12}/2}{RT} + \ln\sqrt{[I_2]} + \ln A'_{12} + \ln A_{13} + \ln t \qquad \text{(eq. 5)}$$

If ln(−ln(1−X)) is plotted against $1/T$, the apparent activation energy, E_a, can be calculated from the slope. The plots based on the DBM conversion data show clean Arrhenius behavior (Figure 4C). E_a was calculated to be 35.9, 36.2, and 35.7 kcal/mol for 1%, 3%, and 5% of the $I_2/(DBM + I_2)$ mole ratio, close to the theoretical value of ($E_{a13} + \Delta H_{12}/2$), which is 39.4 kcal/mol.

Next, we studied the effect of HBr partial pressure. On the basis of our proposed mechanism, HBr is involved in the reaction (rxn. 3). Cofeeding HBr should have an accelerating effect on the overall reaction. This is confirmed by our results (Supporting Information, Figure S8). However, since HBr is generated during the reaction, further increasing the HBr cofeed partial pressure does not lead to significant changes in the conversions.

To further identify the catalytic behavior of iodine in the reaction, we replaced I_2 with other iodo-compounds (CH_2BrI, CH_3I, and C_3H_7I). The conversion and selectivity data are summarized in Figure 5, and the detailed product distributions are given in Supporting Information, Figure S9. Compared to the bromo-compounds studied in this work (Br_2 and $CHBr_3$), which only served as reactants, all the iodo-compounds exhibited a catalytic behavior similar to that of I_2. The iodo-compounds not only increase the conversions of propane and DBM, but also increase the selectivity toward C_3H_6 + C_3H_7X and CH_3Br. The high selectivity can be explained as follows. Thermodynamically (Supporting Information, Figure S1), the driving force for the formation of different products is in the following order: C_3H_6 + HBr + CH_3Br > C_3H_6 + HBr + CH_4 ≫ C_3H_4 + HBr + CH_3Br > C_3H_4 + HBr + CH_4. Kinetically (Figure 6), the energy barrier for

$$\bullet I + CH_3Br \leftrightarrows \bullet CH_3 + IBr \qquad \text{(rxn. 19)}$$

is 28.4 kcal/mol, much higher than that of rxn. 13 (21.1 kcal/mol). According to our estimation, $k_{19} \ll k_{13}$ (Supporting Information,

dx.doi.org/10.1021/cs3001418 | ACS Catal. 2012, 2, 1049−1056

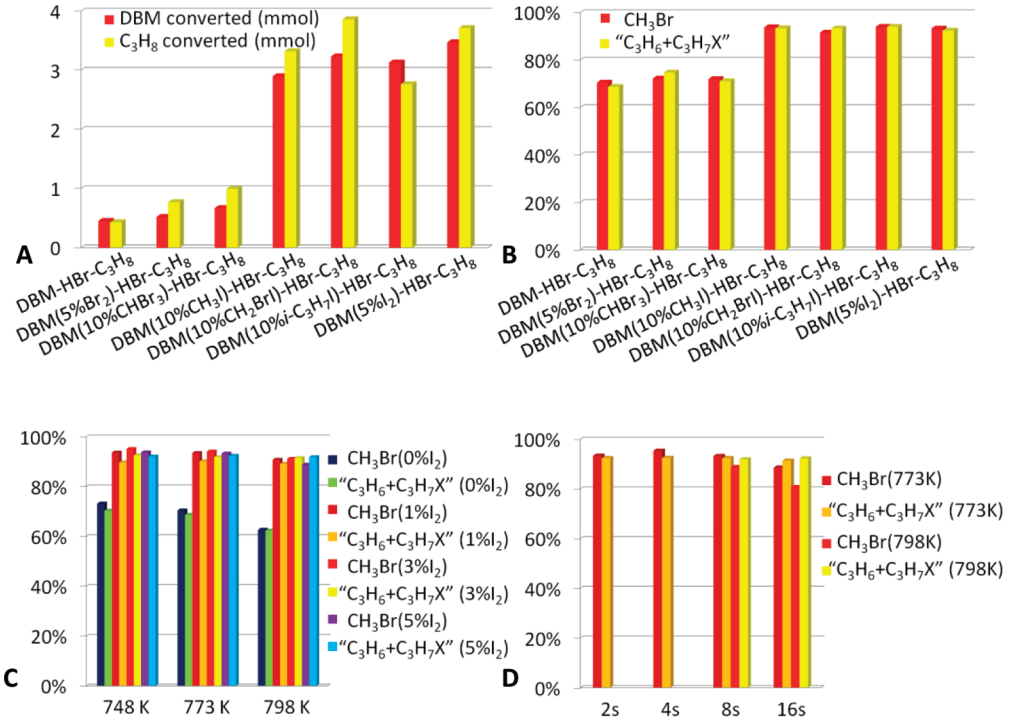

Figure 5. (A) Amounts of converted DBM and C_3H_8; (B) CH_3Br and C_3H_6+C_3H_7X selectivities in the presence of different bromo- or iodo-compounds (773 K, τ = 8 s, CH_2Br_2/C_3H_8/HBr/Ar mole ratio of 7:7:14:33, C_3H_8 input 8.2 mmol); (C) CH_3Br and C_3H_6+C_3H_7X selectivities at different reaction temperatures with different mole ratios of $I_2/(CH_2Br_2 + I_2)$ (τ = 8 s, CH_2Br_2/C_3H_8/HBr/Ar mole ratio of 7:7:14:33, C_3H_8 input 8.2 mmol); (D) CH_3Br and C_3H_6+C_3H_7X selectivities at different reaction temperatures with different residence time (5% of $I_2/(CH_2Br_2+I_2)$, CH_2Br_2/C_3H_8/HBr/Ar mole ratio of 7:7:14:33, C_3H_8 input 8.2 mmol).

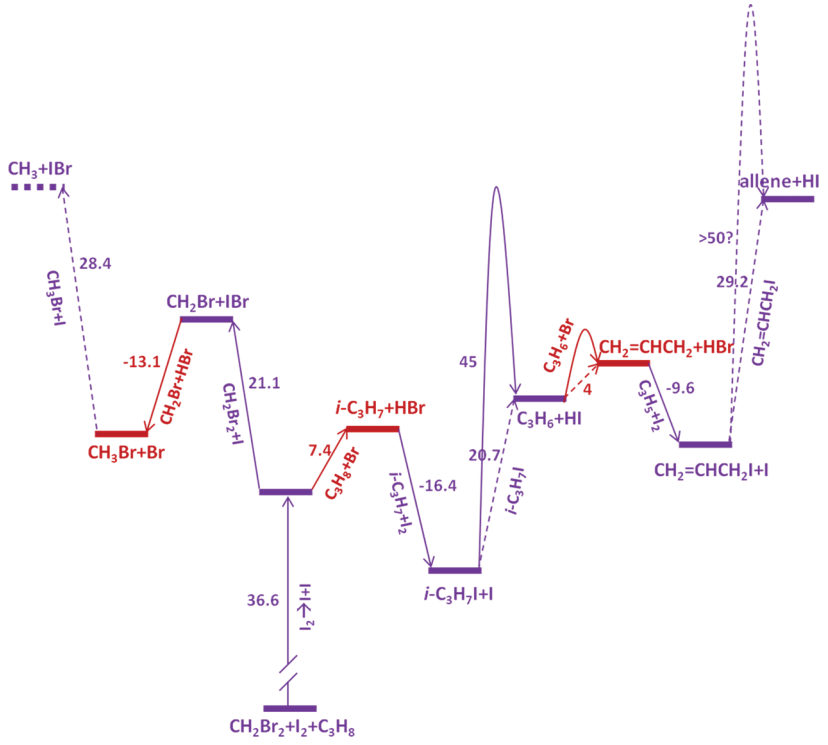

Figure 6. Reaction pathways and energy profile for the formation of CH_4 and allyl-X or allene in "DBM + C_3H_8 + I_2 + HBr + Ar" system.

Table S1). Since rxn. 19 and rxn. 13 are the rate-determining steps for the formation of CH_4 and CH_3Br, the formation rate of CH_4 should be lower than that for CH_3Br unless a very high DBM conversion is achieved.

For the consecutive dehydrogenation of C_3H_6, we know that the allyl C−H bond is weaker than the C−H bonds in C_3H_8, so that H-abstraction from C_3H_6 to form an allyl radical is faster than H-abstraction from C_3H_8 to form the isopropyl radical.

dx.doi.org/10.1021/cs3001418 | *ACS Catal.* 2012, 2, 1049−1056

The allyl radical and isopropyl radical will either be trapped by I_2 to form allyl−I and iso-C_3H_7−I, or abstract H from HBr to convert back to C_3H_6 and C_3H_8 (Figure 6). The elimination of HI from allyl−I is harder than from iso-C_3H_7−I, because the elimination reaction needs to break a β-C−H bond, which is relatively stronger for allyl−I than for iso-C_3H_7−I. However, breaking an allyl−I bond is much easier than breaking an iso-C_3H_7−I bond. Therefore, compared to iso-C_3H_7−I, allyl−I is more likely to dissociate by breaking the C−I bond instead of by the elimination of HI.[26] Basically, the formation of CH_4 and C_3H_4 (or C_3H_5X) is thermodynamically and kinetically unfavorable.

Isotopic tracing experiments were carried out to verify our proposed mechanism. The product distribution from the "CD_2Br_2 + C_3H_8 + I_2 + HBr + Ar" system is given in Supporting Information, Figure S10. 18% of the remaining DBM undergoes a H/D exchange process, which is higher than the H/D exchange observed for methyl bromide. Considering that CH_2DBr might originate from $CHDBr_2$, the degree of H/D exchange was actually much higher for DBM than for methyl bromide. One main reason for this is that the C−D bonds in methyl bromide are stronger than those in DBM. Propane and propylene showed very low degrees of H/D exchange. This is because of the low D content in $H_{1-x}D_xBr$ during the reaction. The degree of H/D exchange for the products from the "CD_2Br_2 + I_2 + HBr + Ar" system were similar with that observed for the "CD_2Br_2 + HBr + Ar" system, however, which is substantially higher than for that found for the "CD_2Br_2 + C_3H_8 + I_2 + HBr + Ar" system (Supporting Information, Figures S11 and S12). This indicates that bromine instead of iodine contributes the most to the H/D exchange process. These results are consistent with our proposed mechanism, in which the dehydrogenation process is mainly driven by bromine radicals.

Our proposed reaction mechanism can be also verified by the kinetic simulations. The simulations were performed using the "Chemical Kinetics Simulator (CKS)" software. Detailed simulation settings including the reaction steps and rate constants are listed in Supporting Information, Table S1. Certain reductions on the reaction steps were introduced to simplify the simulation procedures. Detailed description of the simulation can be found in the Supporting Information. Because of the lack of reported data on rate constants involved in our reaction, some of the rate constants are estimated based on analogous reactions. Most of the reported rate constants were measured in the temperature region of 300−600 K and extending the Arrhenius equation to 800 K might cause certain deviations. Despite these approximations, the general trends of the kinetic behavior should stay the same. This allows us to roughly analyze the kinetic behavior and further compare the differences among different reaction systems.

Supporting Information, Figures S13 and S14 show that DBM slowly disproportionates into CH_3Br and $CHBr_3$ and finally reaches an equilibrated state. Cofeeding HBr accelerates the disproportionation process and leads to more CH_3Br than $CHBr_3$. Considerable bromine formation caused by HBr cofeeding is also confirmed by the simulation (Supporting Information, Figure S14B). The ultraslow kinetic behavior of the "DBM + C_3H_8 + HBr + Ar" system observed in our experiment is reproduced by the kinetic simulation as shown in Supporting Information, Figure S15. Addition of 5% I_2 leads to an approximately 200 times acceleration of the reaction kinetics (Supporting Information, Figure S16). Interestingly, after C_3H_8 reaches 100% conversion, the disproportionation of CH_3Br and CH_2Br_2 takes place. This behavior is reasonable and not unexpected. Supporting Information, Figure S16B shows that the equilibria among I_2, IBr, I, and HI are established immediately at the very early stage of the reaction, and the concentration of all these iodo species remain constant until the conversion of C_3H_8 approaches 100%. The dynamic concentration of the iodine radical is approximately 50 times higher than that of the bromine radical. Combining the rate constants given in Supporting Information, Table S1, we arrive at the following conclusions. The iodine radical contributes more than 20 times what the bromine radical contributes to the bromine abstraction from DBM, while the bromine radical contributes more than 100 times the iodine radical to propane dehydrogenation. Supporting Information, Figures S17 to S19 show that CH_3I, CH_2BrI, and i-C_3H_7I also accelerate the reaction between DBM and C_3H_8, similar to our experimental observations.

CONCLUSIONS

We have demonstrated that a small amount of I_2 can effectively catalyze the gas phase reaction between propane and DBM to produce propylene and methyl bromide. Single-pass "C_3H_6 + C_3H_7X" yields of up to 80% can be easily achieved, and DBM converted to methyl bromide with a highly selectivity. Iodine mainly abstracts bromine out of DBM, while bromine contributes the most to propane dehydrogenation. Our findings are promising for developing an integrated halogen-based pathway to produce propylene from natural gas. On the basis of the current methyl bromide-to-olefin technology, we can integrate a DBM reactor between the methane bromination step and the methyl bromide coupling step. Propane is converted to propylene and DBM is converted to methyl bromide. After passing through a zeolite catalyst, propylene is enriched. Furthermore, the chemistry presented here is a major step in resolving the DBM issue that exists for the current bromine-based GTL technology.[17] Two main side products in the process, DBM from the methane bromination and the paraffins from the coupling, are converted to methyl bromide and light olefins in the presence of iodine. The thermal and mass efficiencies of the overall process can be greatly improved.

ASSOCIATED CONTENT

Supporting Information

Kinetic simulation details, Figures S1−S19, Table S1. This material is available free of charge via the Internet at http://pubs.acs.org.

AUTHOR INFORMATION

Corresponding Author

*E-mail: stucky@chem.ucsb.edu.

Funding

This research was supported by the University of California Discovery Grant Program, GRT Inc., and the U.S. Department of Energy.

Notes

The authors declare no competing financial interest.

ACKNOWLEDGMENTS

We also acknowledge useful discussions with Professor Liming Zhang (University of California, Santa Barbara) and Dr. Peter Stoimenov (GRT, Inc.) regarding the mechanistic interpretation of the results reported in this manuscript.

REFERENCES

(1) TIP Technology Reports. CMAI Global Web site. http://www.cmaiglobal.com/Technology/TechnologyReports.aspx (accessed January 18, 2012).
(2) Crabtree, R. H. *Chem. Rev.* **1995**, *95*, 987−1007.
(3) Kidnay, A.; Parrish, W. R. *Fundamentals of Natural Gas Processing*; Taylor & Francis Group: Boca Raton, FL, 2006.
(4) Bhasin, M. M.; McCain, J. H.; Vora, B. V.; Imai, T.; Pujado, P. R. *Appl. Catal., A* **2001**, *221*, 397−419.
(5) Grabowski, R. *Catal. Rev. - Sci. Eng.* **2006**, *48*, 199−268.
(6) Cavani, F.; Ballarini, N.; Cericola, A. *Catal. Today* **2007**, *127*, 113−131.
(7) Michorczyk, P.; Ogonowski, J. *Appl. Catal., A* **2003**, *251*, 425−433.
(8) Takehira, K.; Ohishi, Y.; Shishido, T.; Kawabata, T.; Takaki, K.; Zhang, Q. H.; Wang, Y. *J. Catal.* **2004**, *224*, 404−416.
(9) Kondratenko, E. V.; Cherian, M.; Baerns, M.; Su, D. S.; Schlogl, R.; Wang, X.; Wachs, I. E. *J. Catal.* **2005**, *234*, 131−142.
(10) Sugiyama, S.; Iizuka, Y.; Nitta, E.; Hayashi, H.; Moffat, J. B. *J. Catal.* **2000**, *189*, 233−237.
(11) Chesnokov, V. V.; Bedilo, A. F.; Heroux, D. S.; Mishakov, I. V.; Klabunde, K. J. *J. Catal.* **2003**, *218*, 438−446.
(12) Mishakov, I. V.; Vedyagin, A. A.; Bedilo, A. F.; Zailovskii, V. I.; Klabunde, K. J. *Catal. Today* **2009**, *144*, 278−284.
(13) Mullineaux, R. D.; Raley, J. H. U.S. Patent 2890253, 1956.
(14) Raley, J. H.; Mullineaux, R. D.; Bittner, C. W. *J. Am. Chem. Soc.* **1963**, *85*, 3174−3178.
(15) Dahl, I. M.; Grande, K.; Jens, K. J.; Rytter, E.; Slagtern, A. *Appl. Catal.* **1991**, *77*, 163−174.
(16) Olah, G. A.; Gupta, B.; Farina, M.; Felberg, J. D.; Ip, W. M.; Husain, A.; Karpeles, R.; Lammertsma, K.; Melhotra, A. K.; Trivedi, N. J. *J. Am. Chem. Soc.* **1985**, *107*, 7097−7105.
(17) Gadewar, S. B.; Wyrsta, M. D.; Grosso, P.; Zhang, A. H.; McFarland, E. W.; Komon, Z. J. A.; Sherman, J. H. U.S. Patent 7579510, 2009.
(18) Butter, S. A.; Jurewicz, A. T.; Kaeding, W. W. U.S. Patent 3894107, 1975.
(19) Olah, G. A.; Doggweiler, H.; Felberg, J. D.; Frohlich, S.; Grdina, M. J.; Karpeles, R.; Keumi, T.; Inaba, S.; Ip, W. M.; Lammertsma, K.; Salem, G.; Tabor, D. C. *J. Am. Chem. Soc.* **1984**, *106*, 2143−2149.
(20) Lersch, P.; Bandermann, F. *Appl. Catal.* **1991**, *75*, 133−152.
(21) Lorkovic, I. M.; Sun, S. L.; Gadewar, S.; Breed, A.; Macala, G. S.; Sardar, A.; Cross, S. E.; Sherman, J. H.; Stucky, G. D.; Ford, P. C. *J. Phys. Chem. A* **2006**, *110*, 8695−8700.
(22) Maccoll, A. *Chem. Rev.* **1969**, *69*, 33−60.
(23) Noller, H.; Kladnig, W. *Catal. Rev. - Sci. Eng.* **1976**, *13*, 149−207.
(24) Nangia, P. S.; Benson, S. W. *J. Am. Chem. Soc.* **1964**, *86*, 2773−2777.
(25) Golden, D. M.; Benson, S. W. *Chem. Rev.* **1969**, *69*, 125−134.
(26) Benson, S. W. *J. Chem. Phys.* **1963**, *38*, 1945−1951.